

On the kinematic signature of a central Galactic bar in observed star samples

P. Vauterin

Royal Observatory of Belgium, Ringlaan 3, B-1180 Brussel, Belgium

H. Dejonghe

Universiteit Gent, Sterrenkundig Observatorium, Krijgslaan 281(S9), B-9000 Gent, Belgium

ABSTRACT

A quasi self-consistent model for a barred structure in the central regions of our Galaxy is used to calculate the signature of such a triaxial structure on the kinematical properties of star samples. We argue that, due to the presence of a velocity dispersion, such effects are much harder to detect in the stellar component than in the gas. It might be almost impossible to detect stellar kinematical evidence for a bar using only l - v diagrams, if there is no a priori knowledge of the potential. Therefore, we propose some test parameters that can easily be applied to observed star samples, and that also incorporate distances or proper motions. We discuss the diagnostic power of these tests as a function of the sample size and the bar strength. We conclude that about 1000 stars would be necessary to diagnose triaxiality with some statistical confidence.

Subject headings: Galaxy: kinematics and dynamics, Galaxy: structure, Galaxy: center, Galaxy: stellar content, methods: statistical

1. Introduction

During the last years, there has been mounting evidence that the central part of our Milky Way contains a triaxial, barlike structure. This theory is supported by the observation of the “parallelogram” structure in the kinematics of the gas (see e.g. Binney et al, 1991), and by the asymmetry in both the integrated light (e.g. Blitz & Spergel, 1991) and the star samples (e.g. Whitelock & Catchpole, 1992).

However, as pointed out already by de Zeeuw (de Zeeuw, 1994), it is striking that there is currently almost no evidence for such a bar in the stellar kinematics. The only observations which seem to point in that direction are the vertex deviations in the samples of K-giants (Zhao, Spergel & Rich, 1994), but these data suffer from large statistical uncertainties. Put differently, triaxial and axisymmetric models fit almost equally well kinematical data (Blum et al., 1995). Of course, this is an unsatisfactory situation, because the stellar component is the most massive one and thus should play a dominant role in the creation and evolution of such a bar.

Therefore, we will address two questions in this paper: (1) which are the dominant effects caused by a triaxial structure in the kinematics of stellar samples, and (2) what is the magnitude of these effects. In this way, we will try to determine where the triaxiality shows up, as well as the required minimal sample size and observational accuracy in order to be able to detect it.

In order to achieve this goal, we use a self-consistent model for the stellar component of a barred galaxy which we developed in an earlier paper (Vauterin & Dejonghe, 1997). The various scale parameters are adjusted in such a way that the model is a fair fit to the central region of our Milky Way. Since the distribution function is known with high accuracy, it is easy to draw synthetic stellar samples from this model.

We discuss the effect of the bar on the l - v diagram, and further construct various test parameters for triaxiality, based on the kinematical properties of individual stars in stellar samples. These tests involve the radial velocities, distances and/or proper motions. Using Monte Carlo simulations, we calculate the distribution of these parameters for different sample sizes, in order to determine minimal sample sizes.

2. A model for the stellar component of a bar in the centre of the Galaxy

We apply a model which we constructed in an earlier paper (Vauterin & Dejonghe, 1997; hereafter paper I). It is based on the nonlinear extension of an unstable linear mode occurring in an initially axisymmetric, two-dimensional model. The galaxy consist of two components:

- An unperturbed, axisymmetric and time-independent part with a binding potential V_0 and a distribution function f_0 . The parameters (scale and rotation curve) are adjusted in order to fit the central region of the Galaxy. The rotation curve of this model is displayed in fig. 1, and additional details about this model can be found in paper I.
- A barlike perturbation, which is non-axisymmetric and time-dependent. The binding potential is denoted by V' , and the distribution function is f' . The time and angular dependency of this part are of the following form:

$$\Re \left[e^{i(m\theta - \omega t)} \right], \quad (1)$$

where m is the symmetry number, $\Re(\omega)/m$ the rotation speed and $\Im(\omega)$ the growth rate.

The motion of the stars in the perturbation is a solution of the Boltzmann equation:

$$\frac{\partial f'}{\partial t} - [f'_0, V'] = [f_0, V'] + [f', V']. \quad (2)$$

In addition, for a self-consistent perturbation, the Poisson equation applies:

$$\nabla V' = 4\pi G \rho'. \quad (3)$$

When the perturbation is sufficiently small, one can linearize the equations. In this case, the last, quadratic term of the Boltzmann equation is omitted. Solutions (V', f') that satisfy both the Poisson equation and the linearized Boltzmann equation are called linear modes. There exist various methods in the literature to solve this problem (e.g. Kalnajs, 1977, Hunter, 1992, Vauterin & Dejonghe, 1996). The analyses show that, for each value of m , an infinite series of linear modes exists, with different rotation speeds and growth rates. The mode with the highest growth rate is the dominant instability. In most

cases, it turns out to be an $m = 2$ barlike structure (as is the case for the present model).

By construction, linear modes are only valid for infinitesimally small amplitudes of the perturbation. In order to construct finite amplitude perturbations, we performed a nonlinear extension. The total potential is taken from the linear mode, $V_{\text{TOT}} = V_0 + \epsilon V'$, but the corresponding distribution function is obtained by solving the full, nonlinear Boltzmann equation numerically. The details about these calculations are given in paper I.

The total distribution function of such a barred model can be accurately calculated for any point in phase space. In addition, it is possible to calculate derived quantities, such as mass densities, streaming velocities, etc., by numerical integration over a grid in the velocity coordinates

In this way, we constructed a physically meaningful barred model, which is self-consistent to a large degree. The bar has a semi-major axis of about 2 kpc, a semi-minor axis of about 1 kpc, and has a 15 degrees tilt angle with respect to the direction of the sun. In addition, we have put the sun at a distance of 8 kpc from the center of the Galaxy. These values seem to be more or less compatible with most of the observations (see e.g. Zhao, 1994).

3. Stellar l - v diagrams of the bar

In the top panels of fig. 2, we compare the stellar l - v diagram of the barred model to the one of the unperturbed system. Apart from density changes, the presence of the bar also clearly has some effects on the kinematical properties of the l - v diagram. The most important difference is that the average radial velocity of the stars is higher than the rotation curve of the axisymmetric potential. This is easily explained by the fact that we see the bar almost along the major axis, and that the stars crossing the minor axis are moving faster than those crossing the major axis of the bar (see e.g. fig. 7 of paper I). The same figure also shows the l - v diagram of the barred model, observed from different points. The presence of a bar also clearly introduces substantial changes in the structure of these diagrams.

However, if the potential is not known a priori, it is not possible to easily conclude that these l - v diagrams are caused by a barred system. They could very well be compatible with an axisymmetric system that has a steeper or a slower rotation curve. There-

fore, the l - v diagram alone is usually not sufficient to prove triaxiality, and one needs to incorporate other information as well. This is in contrast to the situation for the gas, where the bar introduces orbits that are “forbidden” by an axisymmetric potential. Unfortunately, there exist no such forbidden regions for stars, due to the presence of a velocity dispersion.

In addition, the features induced by triaxiality are much less pronounced in the stellar l - v diagram than in the gaseous counterpart. Again, this is mainly due to the important velocity dispersion of the stars, which tends to smooth out the various properties of the different orbital families (see also paper I). The situation for the gas is much simpler, since, in a good approximation, the behaviour of the system at each point is completely determined by the single, closed orbit passing through that point.

4. Tests including additional information

As mentioned in the previous section, the galactic length l and the radial velocity v_r of the stars in a sample are not sufficient to make a clear distinction between a triaxial and an axisymmetric system. Therefore, we will investigate two additional types of information: distances and proper motions. It is well known though that such information, if present at all, is subject to rather large errors. A test should therefore not rely too critically on the exact values of these quantities, but should be rather robust to errors.

In fig. 3, the streaming velocities of the stars in a barred system are shown in an exaggerated and schematic way. The streamlines have an elliptical form, aligned along the major axis of the system. In addition, the mean velocity is larger for stars that cross the minor axis than for those on the major axis. It is clear that tests for triaxiality should take advantage of these properties in some way.

The test parameters presented in the following sections are functions of the observable parameters of a star sample taken from the centre of our Galaxy. Therefore, we need simulated star samples, in order to be able to discuss the properties of these parameters. One can easily draw such a star sample from the stellar distribution function using a try-and-reject technique. In this approach, a random number generator creates star coordinates (positions \vec{r} and velocities \vec{v} , both in rectangular reference systems) that have a rectangular distribution over the whole area of interest. For each star, an additional random number R is

further generated, having a rectangular distribution between 0 and the maximum value reached by distribution function (for our models, this corresponds to the central value). The coordinates (\vec{r}, \vec{v}) are accepted as a new member of the star sample only if the value of R is smaller than the value of the distribution function at that point; it is rejected in the other case. This process is continued until the sample contains the desired number of stars.

4.1. Distance information and radial velocities

As shown in fig. 3, the line of zero mean line-of-sight (LOS) velocity in a barred system with the adopted orientation is in general not aligned anymore with the line $l = 0$ (as is the case for an axisymmetric system). As a consequence, there is a symmetry breakdown in the l - v diagram: the part of the diagram that contains stars that are closer to the sun than the galactic centre is not identical anymore to the part that contains the stars lying farther away.

In this section, we will exploit this asymmetry, and use it as a basis for a test parameter for the triaxiality of the system. To this end, we subdivide the stars into eight different groups, labelled (xxx) , where x can be $-$ or $+$ (see also fig. 4). The first sign indicates the distance from the sun ($-$ means closer than the galactic centre and $+$ means further away), the second sign is related to the galactic longitude ($-$ for negative and $+$ for positive longitudes), and the last sign is determined by the radial velocity ($-$ for negative values and $+$ for positive values).

The number of stars N_{xxx} in each subclass is used in order to construct a test parameter:

$$T_1 = \frac{1}{2} \left(\frac{N_{--+} / N_{---}}{N_{-+-} / N_{-++}} + \frac{N_{++-} / N_{+++}}{N_{+-+} / N_{++-}} \right) \times 100. \quad (4)$$

The denominators of both fractions contain the fraction of counterrotating stars in the minor axis quadrants, at the near side (first fraction), and at the far side (second fraction). On the other hand, the numerators contain the fraction of counterrotating stars in the major axis quadrants in the corresponding distances classes. Therefore, this parameter essentially expresses the fact that the quadrants containing the major axis of the bar (i.e. N_{-+x} and N_{+-x}) contain more counterrotating stars than the other quadrants (N_{++x} and N_{--x}).

Because we take only ratios of stars in one give distance class, the parameter is insensitive to photometric effects (caused by the fact that there is a bias against seeing stars at the far side of the bar), and is thus mostly determined by the kinematical properties of the sample. It only requires crude distance information, which is a prerequisite condition since distances are usually subject to large errors.

It is important to notice that large numbers of stars are summed in each subclass, resulting in reduced noise effects. In addition, it is a so-called "robust" test parameter, because only numbers of stars are involved instead of measured values. Such a parameter is relatively insensitive to outliers.

4.2. Proper motions

A second test only involves proper motions. It is based on the fact that, in a barred system which is not aligned with the line of sight, the mean proper motions for positive and negative galactic longitudes have opposite sign (see also fig. 3 and fig. 5). This asymmetry is quantified using a second test parameter, which measures the difference in proper motion (PM) at positive and negative galactic longitudes.

$$T_2 = \langle PM_{l>0} \rangle - \langle PM_{l<0} \rangle. \quad (5)$$

Unfortunately, this parameter is not robust with respect to errors in the observed proper motions, so it might be less useful in practical circumstances.

4.3. Proper motions and radial velocities

It also follows from fig. 3 that, in a barred system that is not aligned with the direction of the sun, the line of zero LOS velocity is not equal to the $l = 0$ line (as is the case for axisymmetric systems). This phenomenon causes differences in the partial l - v diagrams containing stars with respectively only positive and negative proper motions. In order to quantify this difference, two subsets are drawn from the star sample: (1) stars having positive proper motions and lying in the upper 25% of the proper motion distribution, and (2) stars having negative proper motions and lying in the lowest 25%. We rejected the middle 50%, because this is the "gray area", where large measurement errors cause uncertainties on the sign of the proper motion. Fig. 6 displays the l - v diagrams of both subsets, and shows that the first subset has, on average, larger radial velocities than the second.

This difference is measured by the third test parameter, defined as the difference between the mean radial velocities of both subsets:

$$T_3 = \langle v_r, pm > 75\% \rangle - \langle v_r, pm < 25\% \rangle. \quad (6)$$

Again, this test parameter turns out to be fairly insensitive to photometric effects. It is also robust with respect to errors on the measurement of proper motions, since it depends only on their sign rather than on their exact values. The fact that it is not robust with respect to the radial velocities is not a disadvantage, because these values can be measured with rather high accuracy.

As one can infer from fig. 3, the symmetry breakdown of the radial motions and the proper motions turn out to work in the same direction for the value of T_3 . Obviously, this effect has a positive influence on the discriminating power of this parameter.

4.4. Monte Carlo simulations of the test parameters

We used a Monte-Carlo simulation technique to numerically calculate the statistical distributions of the test parameters for a given galaxy model. A large set of random star samples, consistent with the distribution function of the model, is constructed, and the values of the various test parameters are calculated for each individual sample. The parameter values of all samples are further binned into a histogram in order to calculate a numerical estimate of the distributions of these parameters. Obviously, one should incorporate a sufficient number of synthetic samples in order to obtain a histogram with enough resolution. We use histograms with 10 intervals, and a simulation set containing 100 samples for each model. We have checked that this number is sufficient to obtain a reasonable degree of accuracy by checking the consistency of the results with estimations based on larger simulation sets.

4.5. Probability distribution functions of the test parameters

We calculated the distribution function of the parameters T_1 , T_2 and T_3 for two different galaxy models: an axisymmetric one and a barred system with parameters adjusted to those of our Milky Way. These distribution functions were calculated for samples containing 700 and 1400 stars. The resulting distributions are shown in fig. 7.

4.5.1. Verification of a hypothesis using observed data

The combination of part [2] and [3] of the histogram (part [2] is the overlap between both distributions) gives the probability distribution for the parameters in the case of an axisymmetric model. If one has calculated a test parameter using actual observations of our Milky Way, the corresponding distribution can be used to check whether the value is consistent with an axisymmetric model or not, given a specified level of confidence.

On the other hand, part [1] and [2] correspond to the probability distribution for the parameters of the barred model. Again, when actual observations are present, this curve can be used to check the consistency with this model.

4.5.2. Determination of the resolving power of a test parameter

One can use the information in fig. 7 to estimate the diagnostic power of a particular test for a given sample size. Let assume that, in reality, the centre of our Milky Way is barred and more or less consistent with our model. Suppose further that one wants to be able to reject the null hypothesis (“an axisymmetric system”) with a specified confidence level α (e.g. 95%). To this end, any observed test parameter has to lie outside the $1 - \alpha$ region of the probability curve of the axisymmetric model [2]+[3]. Since we assumed that the galaxy is compatible with the barred model, we know a priori that this parameter obeys the distribution [1]+[2]. Using this information, one can calculate the probability that the parameter indeed lies outside this region.

In fig. 8, the probabilities for rejection of the null hypothesis are shown for several confidence levels, as a function of the strength of the bar (a value of 1 corresponds to the model described in section 2). These results are calculated using Gaussian fits to the distributions of the test parameters. The estimates for bar strengths other than 1 are based on a linear interpolation of the parameter distributions between the axisymmetric and the barred model. This approximation is justified by the fact that our model is to a high degree linear, and that the test parameters of both extreme models have more or less the same distribution. Of course, one should realize that these numbers are based on a limited number Monte-Carlo simulations, and these values should therefore be considered only

as rough estimates.

The third test parameter clearly turns out to be the most discriminating one. Presumably, this is a consequence of the fact that the deviation of the proper motions and the radial velocities happen to work in the same direction. For samples containing 700 stars, it is the only test that offers a reasonable chance to rule out an axisymmetric model at a high level of confidence. The first test turns out to be less sensitive, but still offers a reasonable discriminating power for samples containing (at least) 1400 stars. The second test, which only involves proper motions, has the poorest score.

These probability numbers indicate the a priori chance that a particular type of observations will lead to positive results. In this way, they are very useful for the estimation of the required sample size.

5. Conclusions

Although many observations point in the direction of a triaxial structure in the central region of our Galaxy, there has been so far very little evidence for this in the kinematical properties of the stars. In section 3, we have shown that, to a large degree, this can be explained by the presence of a velocity dispersion in the motion of the stars. Such a dispersion diminishes the effects of the bar on the distribution function, by “smearing them out” over a large portion of phase space. As a consequence, it turns out to be very hard to prove triaxiality from an l - v diagram alone, even if a very large number of stars is involved, unless one has some additional information concerning the potential, obtained in an other way.

In the remainder of the article, we have shown that if distances and/or proper motions of the stars are known, it is possible to construct test parameters which discriminate between axisymmetric and triaxial models. Because distances and proper motions are usually subject to large errors, the tests were designed to be “robust” with respect to these values. Moreover, the use of only first order moments has a distinct advantage over second order moments (on which e.g. vertex deviation is based), because higher order moments are less well constrained by the data. Monte-Carlo simulations were further used in order to estimate the probability distribution function of these test parameters for different models. It turns out that the most powerful test incorporates a combination of radial velocities and proper motions. However, even

in this case, one needs a large sample size (of the order of 1000 stars) in order to have a good chance to be able to rule out an axisymmetric model with a high degree of confidence.

REFERENCES

- Binney, J.J., Gerhard, O.E., Stark, A.A., Bally, J., Uchida, K.I., 1991, MNRAS, 252, 210
- Blitz, L., Spergel, D.N., 1991, ApJ, 379, 631
- Blum, R. D., Carr, J. S., Sellgren, K., Terndrup, D. M., 1995, ApJ, 449, 623
- Hunter C., 1992, in Hunter J.H., Wilson R.E., eds, Astrophysical disks, New York Academy of Sciences
- Kalnajs A. J., 1977, ApJ, 212, 637
- Vauterin P., Dejonghe H., 1996, A & A, 313, 465
- Vauterin P., Dejonghe H., 1997, MNRAS, 286, 812
- Whitelock, P.A., Catchpole, R.M., 1992, in The center, Bulge and Disk of the Milky Way, ed. Blitz, L. Kluwer, Dordrecht, p. 103
- de Zeeuw T., 1993, in Galactic Bulges, eds. Dejonghe H., Habing H.J. Kluwer, Dordrecht, p. 191
- Zhao, H., 1994, PhD Thesis, Columbia University
- Zhao H., Spergel D. M., Rich R. M., 1994, AJ, 106, 2154

Fig. 1.— Rotation curve, mean velocity and dispersions of the axisymmetric model.

Fig. 2.— l - v diagrams of the barred model (top left) and the unperturbed system (top right). The axisymmetric rotation curve is indicated by the white line. The mass distribution and the orientation of the observer of the system is shown in the small pictures. The bottom row shows the same bar with different orientations.

Fig. 3.— Schematic view of the streaming velocities in a barred stellar system. Note the counterrotating streamlines that are present in the quadrants containing the major axis. This is in contrast to axisymmetric systems, where counterrotating stars are present only because of velocity dispersion.

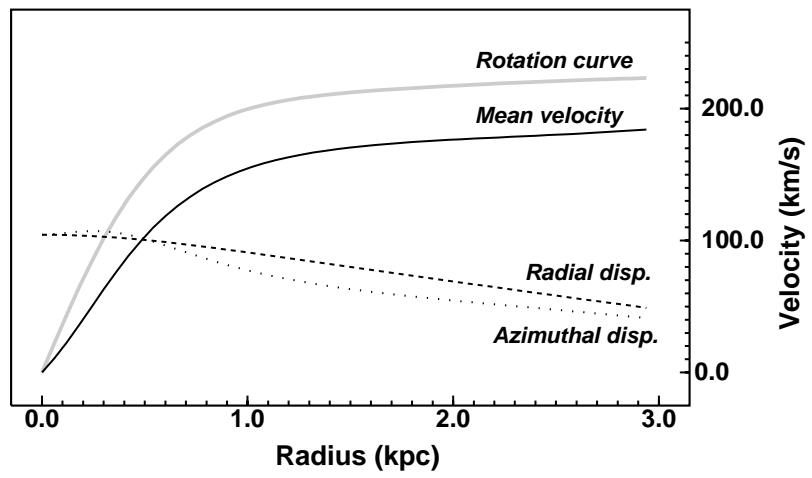
Fig. 4.— The l - v diagrams of a simulated star sample, drawn from the barred model, for stars further away than the galactic centre (top panel), and stars closer to the sun (bottom panel). The gray curves represent the axisymmetric rotation curve, and in each quadrant of the graphs, the corresponding subsample index is marked (see text). The star sample contains 700 stars.

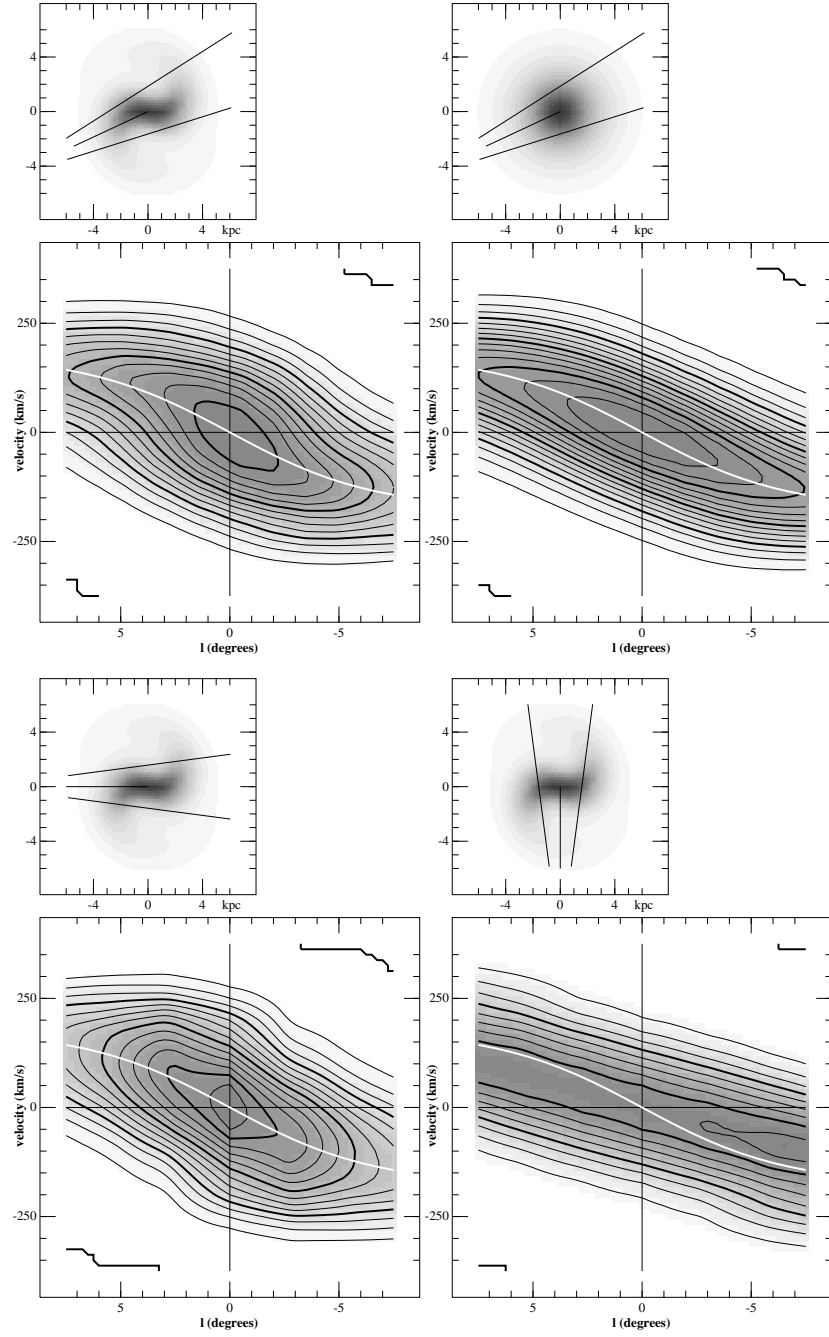
Fig. 5.— Proper motions of a simulated star sample (drawn from the barred model) as a function of the galactic length. The gray line indicates the averaged values.

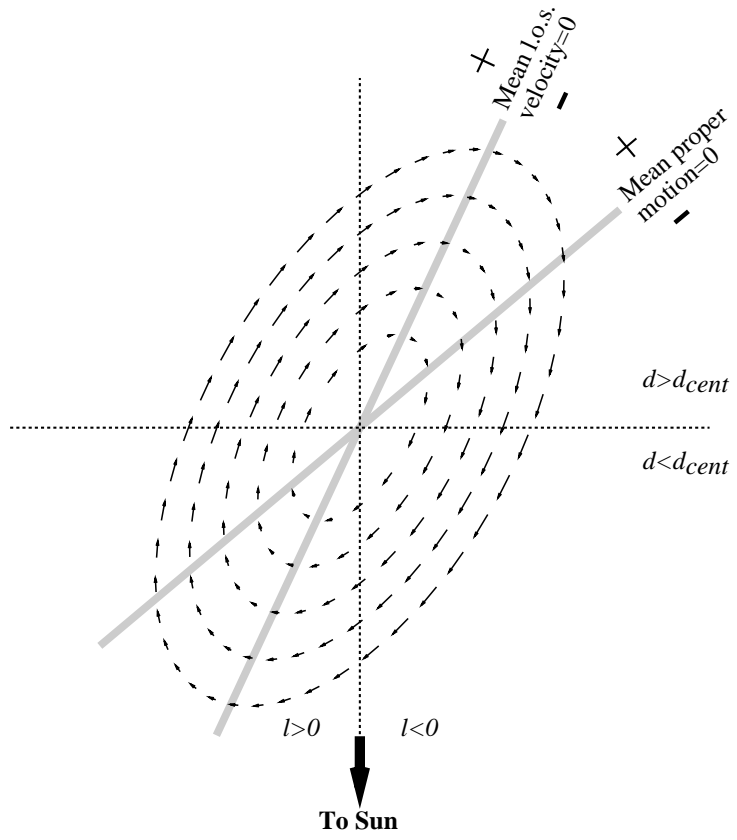
Fig. 6.— The l - v diagrams of a simulated star sample for the upper 75% subset (top panel) and the lower 25% (bottom panel). The sample contains 700 stars, and is drawn from the barred model. The gray lines indicate the axisymmetric rotation curve.

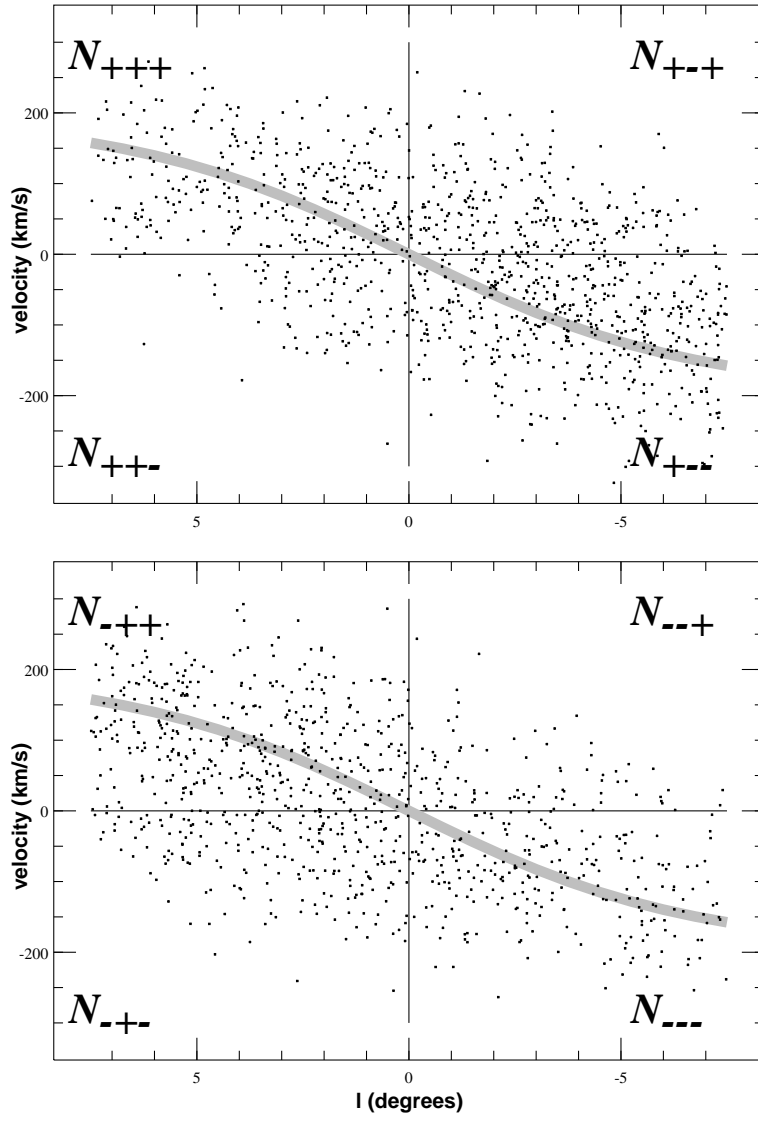
Fig. 7.— Distribution functions of the test parameters for different models.

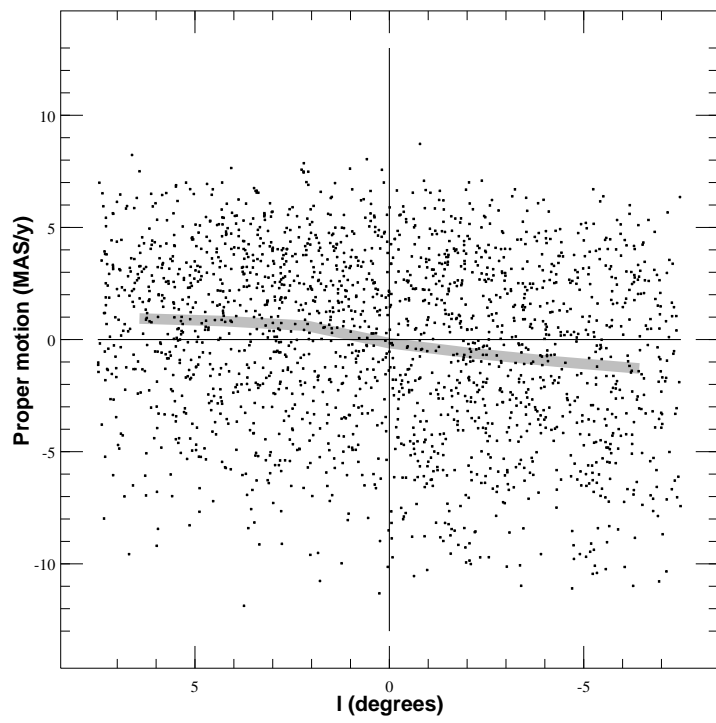
Fig. 8.— Probabilities for rejection of the axisymmetric hypothesis for the three test parameters, at different levels of confidence, and for various bar strengths (expressed as a fraction of the strength of the bar in our model).



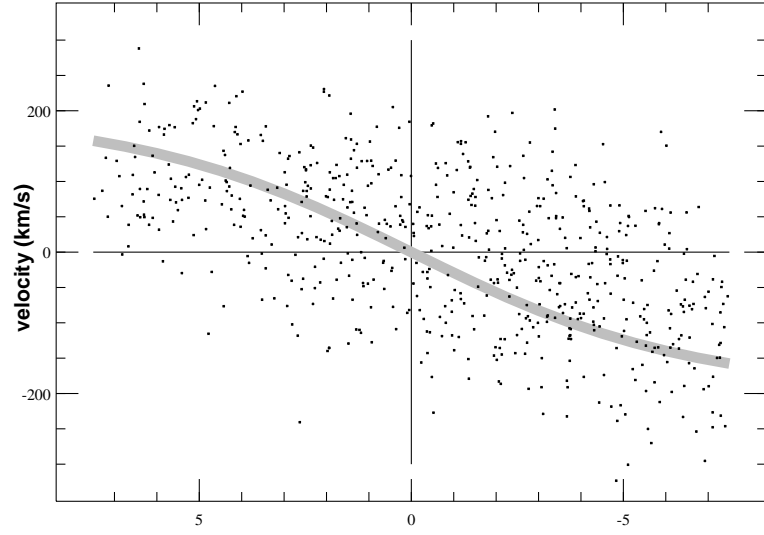








pm > 75%



pm < -75%

